

# Geophysical Research Letters



## RESEARCH LETTER

10.1029/2020GL092142

## How Does the North Atlantic SST Pattern Respond to Anthropogenic Aerosols in the 1970s and 2000s?

### Key Points:

- Anthropogenic aerosol patterns affect the coupled atmosphere-ocean dynamical response
- 1970s to 2000s aerosol pattern change enhances North Atlantic warming hole through ocean meridional heat convergence by the sub-polar gyre
- Most of the response to anthropogenic aerosols is associated with aerosol-cloud interactions

### Supporting Information:

- Supporting Information S1

### Correspondence to:

S. Fiedler,  
[stephanie.fiedler@uni-koeln.de](mailto:stephanie.fiedler@uni-koeln.de)

### Citation:

Fiedler, S., & Putrasahan, D. (2021). How does the North Atlantic SST pattern respond to anthropogenic aerosols in the 1970s and 2000s? *Geophysical Research Letters*, *48*, e2020GL092142. <https://doi.org/10.1029/2020GL092142>

Received 17 DEC 2020  
Accepted 21 FEB 2021

S. Fiedler<sup>1,2,3</sup>  and D. Putrasahan<sup>4</sup> 

<sup>1</sup>Institute for Geophysics and Meteorology, University of Cologne, Cologne, Germany, <sup>2</sup>Hans-Ertel-Centre for Weather Research, Climate Monitoring and Diagnostics, Bonn/Cologne, Germany, <sup>3</sup>Previously: Max-Planck-Institute for Meteorology, Atmosphere in the Earth System, Hamburg, Germany, <sup>4</sup>Max-Planck-Institute for Meteorology, Ocean in the Earth System, Hamburg, Germany

**Abstract** We show how changes in the global distribution of anthropogenic aerosols favor different spatial patterns in the North Atlantic sea-surface temperature (NASST). The NASSTs largely show the expected decrease associated with the anthropogenic aerosols in the 1970s, but also an unusual warming response in the eastern sub-polar gyre, the region of the North Atlantic warming hole. The NASST response reversed for the anthropogenic aerosols in the 2000s against 1970s. The regional reduction in anthropogenic aerosols favored as follows: (1) a strengthening of the warming hole and (2) a NASST increase at high latitudes associated with changes in the coupled atmosphere-ocean dynamics. We found that the gyre component of the northward Atlantic heat transport in mid-to high latitudes is an important driver for the heat convergence associated with the NASST patterns. At least two-thirds of the NASST response in MPI-ESM1.2 is associated with aerosol-cloud interactions, highlighting the need to better understand them.

**Plain Language Summary** The change of the North Atlantic sea-surface temperature due to anthropogenic aerosols is not well understood. Aerosols reflect incoming solar radiation and influence clouds. Both effects are expected to cool the surface. The expected surface cooling (warming) due to more (less) aerosols is mostly seen in our experiment, but we also find an unusual warming (cooling) in a region in the North Atlantic, where observations show no clear warming trend. We identify that this area, known as the North Atlantic warming hole, is affected by circulation changes that are induced by the aerosol changes between the pre-industrial, the 1970s and the 2000s. Changes of the heat transport in the ocean from the warming hole to the Arctic drives these changes. The magnitude of this temperature change in our experiments largely depends on the still uncertain aerosol effect on clouds.

## 1. Introduction

Patterns in the North Atlantic sea-surface temperature (NASST) change over time. Observations indicate a clear change from negative NASST anomalies in the 1970s–1990s to positive anomalies in more recent decades (Enfield et al., 2001; Trenberth & Shea, 2006), superimposed on the positive global trend in NASSTs associated with the increase in atmospheric greenhouse gas concentrations (IPCC, 2013). We illustrate the global pattern of NASST differences with results from the historical simulations of the Max Planck Institute-Earth System Model (MPI-ESM1.2; Figures S1a and S1b), using transient changes in atmospheric composition of the Coupled Model Inter-comparison Project phase six (CMIP6, Eyring et al., 2016). While most ocean regions show the expected warming due to greenhouse gas forcing since the pre-industrial, the sub-polar gyre in the North Atlantic stands out with a cool anomaly, known as the North Atlantic warming hole (NAWH, e.g., Drijfhout et al., 2012; Gervais et al., 2016; Marshall et al., 2015; Rahmstorf et al., 2015; Woollings et al., 2012; Figure S1a). Relative to the 1970s, the NAWH changed little while the northern hemisphere in the 2000s generally warmed more than the southern hemisphere (e.g., Figure S1b). Despite the importance of understanding near-surface warming patterns, the underlying physical mechanisms of the NASST patterns are still poorly understood, so much so that different plausible explanations exist (e.g., Booth et al., 2012; Clement et al., 2015; Dagan et al., 2020; Delworth & Mann, 2000; Keil et al., 2020; Kim et al., 2018; Otter et al., 2010; Wang et al., 2012).

© 2021. The Authors.

This is an open access article under the terms of the [Creative Commons Attribution-NonCommercial-NoDerivs License](https://creativecommons.org/licenses/by-nc-nd/4.0/), which permits use and distribution in any medium, provided the original work is properly cited, the use is non-commercial and no modifications or adaptations are made.

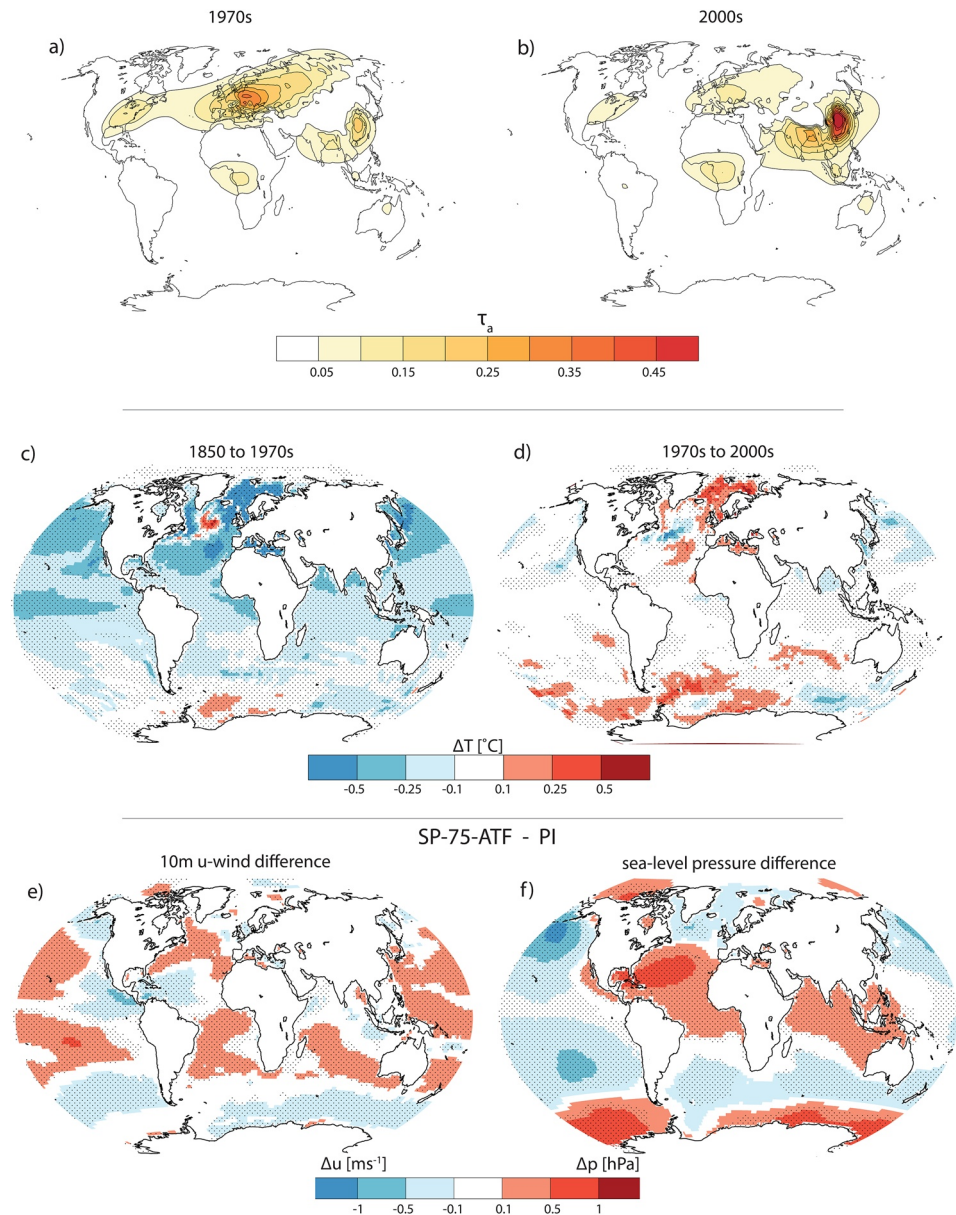


**Figure 1.** Anthropogenic aerosol optical depth and climate response. Shown are the mean anthropogenic aerosol optical depth ( $\tau_a$ ) for the (a) 1970s and (b) 2000s, the response of the climatological mean sea-surface temperature ( $\Delta T$ ) to  $\tau_a$  of (c) the 1970s (SP-75) against 1850 (PI) and (d) the 2000s (SP-05) against the 1970s (SP-75), as well as the response of (e) the zonal wind component at 10 m ( $\Delta u$ ) and (f) the mean sea-level pressure ( $\Delta p$ ) to the 1970s aerosol pattern with enhanced  $\tau_a$  (SP-75-ATF) compared to 1850 (PI). Dotted areas in c–f mark statistically significant results, adopting a confidence level of 5%. Results are based on 200-years of model output that account for aerosol-radiation interaction, the Twomey effect, rapid adjustments, and slow responses.

Booth et al. (2012) concluded that the reduction of anthropogenic aerosol concentrations over the North Atlantic plays a role in reproducing the temperature changes with their CMIP5 model HadGEM2-ES. Anthropogenic aerosols reduce the incoming shortwave radiation at the surface through scattering and absorption, termed aerosol-radiation interaction (ARI), as well as through aerosol effects on clouds, known as aerosol-cloud interaction (ACI). The magnitude of the associated radiative forcing is much debated, but an agreement is that the uncertainty in ARI is smaller than in ACI (Bellouin et al., 2020). The lower anthropogenic aerosol optical depth ( $\tau_a$ ) over the North Atlantic in the 2000s (Figure 1a) is associated with less incoming shortwave radiation being scattered back to space compared to the 1970s. The less negative radiative

effects in the 2000s relative to the 1970s over the North Atlantic (Figure 1b) suggest an accelerated warming during this period. For instance, temperature observations over land support such an accelerated warming since the 1970s after a multi-decadal period of global dimming by anthropogenic aerosols (Wild, 2009).

This idea of changes in NASST patterns being a forced response to anthropogenic aerosol forcing (e.g., Bellucci et al., 2017; Booth et al., 2012; Dagan et al., 2020) seems at odds with another scientific perception, namely that natural variability internal to the system drives NASST anomalies. One example is the study by Delworth and Mann (2000) identifying NASST anomalies much earlier in the history with data of the past 330 years. Since part of this data includes the pre-industrial era when anthropogenic aerosol burden was much lower than today, it suggests that anthropogenic aerosol changes alone cannot be the full explanation of changes in NASST patterns. However, this does not preclude to anthropogenic aerosol not having an influence on atmosphere-ocean dynamics and consequently, NASST patterns. Past studies linked changes in the NASST pattern with differences in the AMOC (e.g., Delworth & Mann, 2000; Drijfhout et al., 2012; Knight et al., 2005). When the AMOC is relatively strong, the North Atlantic becomes anomalously warm due to a stronger northward heat transport, corresponding with a warm phase of the North Atlantic. In response of the positive SST anomaly in the polar North Atlantic, ocean convection reduces and leads to a subsequent weakening of the AMOC. Since now less heat is transported northwards, a cool phase of the North Atlantic develops (e.g., Knight et al., 2005; Zhang & Wang, 2013). Given the different perceptions, it is no surprise that the idea of an AMOC response to aerosol changes receives ongoing attention, for example, studies parallel to ours exploited the CMIP6 historical simulations to investigate the AMOC response to aerosol changes (Hassan et al., 2020; Menary et al., 2020).

In light of these two seemingly different explanations for the drivers of NASST patterns, we here revisit the response of NASSTs to anthropogenic aerosols in the 1970s and 2000s in order to reconcile the different perspectives. The general idea of a NASST response to aerosols is not new, but we present a first systematic assessment of the NASST response to the anthropogenic aerosol patterns with particular attention to the counter-intuitive response in the NAWH using the current knowledge of uncertainty in the magnitude of anthropogenic aerosol radiative effects and applying diagnostics for individual processes in the fully coupled atmosphere-ocean dynamics. To this end, we perform new several hundred years of climate simulations for every aerosol pattern with different forcing magnitudes. This strategy eliminates the impact of model-internal variability on the NASST. Our assessment is guided by the following hypotheses:

1. *The anthropogenic aerosol pattern of the 1970s leads to a stronger cooling response in the North Atlantic than the aerosols of the 2000s.* We expected it due to the more negative radiative effects for the 1970s over the North Atlantic in five contemporary climate models (Fiedler et al., 2019b) and the paradigm change from global dimming to brightening in observations (IPCC, 2013; Wild, 2009)
2. *Uncertainty in ACI dominates the strength in the NASST response to anthropogenic aerosols.* This is motivated by the current knowledge of the uncertainty in the magnitude of ACI that is larger than the one for ARI (Bellouin et al., 2020), ACI being more important for the AMOC response (Menary et al., 2020), and the case of the CMIP5 model HadGEM2-ES (Booth et al., 2012). HadGEM2-ES has a relatively strong radiative forcing of anthropogenic aerosols (Bellouin et al., 2011) and has been used to argue that the historical forcing of anthropogenic aerosols is important for reconstructing the development of NASSTs (Booth et al., 2012)
3. *Coupled dynamical ocean-atmosphere response to anthropogenic aerosols influences NASST response.* We postulate that anthropogenic aerosols can exert an influence on both the atmosphere and ocean, for which the ocean response can superimpose on naturally occurring oceanic drivers of NASST. The hypothesis is based on competing theories about the origins of NASST variability in past studies and the identification of NASST anomalies in the pre-industrial era (e.g., Booth et al., 2012; Clement et al., 2015; Delworth & Mann, 2000; Kim et al., 2018), when  $\tau_a$  was low and is therefore eliminated as sole driver of NASST anomalies. Our idea is consistent with previous works to the extent of the assessment of the thermohaline circulation (Cai et al., 2006; Cowan & Cai, 2013; Delworth & Dixon, 2006; Hassan et al., 2020; Menary et al., 2020) and parallel work on the NAWH with other data (Dagan et al., 2020), but these studies did not investigate the fully coupled atmosphere-ocean dynamical response to the anthropogenic aerosols of the 1970s and 2000s separating model-internal variability and components of the ocean meridional heat transport

**Table 1**  
Overview on Model Experiments<sup>a</sup>

Experiment setup			Global oceans			North Atlantic		
Name	$t_{ARI}$	$t_{ACI}$	$\tau_a$	$F$ ( $Wm^{-2}$ )	$\Delta T$ ( $^{\circ}C$ )	$\tau_a$	$F$ ( $Wm^{-2}$ )	$\Delta T$ ( $^{\circ}C$ )
PI	1850	1850	0	0	0	0	0	0
SP-05	2005	2005	0.01	-0.36	-0.18	0.02	-0.84	-0.27
SP-75	1975	1975	0.01	-0.31	-0.18	0.04	-1.42	-0.28
SP-75-NT	1975	1850	0.01	-0.06	-0.05	0.04	-0.43	-0.09
SP-75-ATF	1975 <sup>b</sup>	1975 <sup>b</sup>	0.03	-0.55	-0.26	0.18	-3.38	-0.54

<sup>a</sup>Listed are the chosen years for the aerosol-radiation interaction ( $t_{ARI}$ ) and aerosol-cloud interaction ( $t_{ACI}$ ) in MACv2-SP as well as the anthropogenic aerosol optical depth ( $\tau_a$ ), the equilibrium radiative forcing ( $F$ ) and the SST response ( $\Delta SST$ ) averaged over global oceans and the North Atlantic ( $80^{\circ}W-0^{\circ}$ ,  $0^{\circ}-60^{\circ}N$ ). <sup>b</sup>Marks larger  $\tau_a$ , but identical spatial distribution as of the year 1975.

We introduce the experiment strategy to test the hypotheses in Section 2, followed by the results (Section 3) and their discussion (Section 4), and draw conclusions at the end (Section 5).

## 2. Experiment Strategy

We perform a suite of new experiments using the CMIP6 configuration of MPI-ESM1.2 (Mauritsen et al., 2019). A main difference between MPI-ESM1.2 and previous model versions is the implementation of the novel simple plumes parameterization, MACv2-SP (Fiedler et al., 2017; Stevens et al., 2017), for optical properties of anthropogenic aerosols and an associated effect on the cloud albedo. Comprehensive evaluations of MPI-ESM1.2 against observations and other climate models have previously been conducted (e.g., Fiedler et al., 2019b; Maher et al., 2019; Mauritsen et al., 2019).

Our experiment strategy is different from previous works to eliminate the impact of model-internal variability on the magnitude of the SST response, that is, we perform five fully coupled atmosphere-ocean simulations (Table 1) with each integrated for 250 years. Each experiment setup uses the same initial and annually repeating boundary data, except for the anthropogenic aerosols. Experiment PI has no anthropogenic aerosol and is our pre-industrial (1850) reference simulation. All other experiments use prescribed annually repeating monthly means of anthropogenic aerosol optical properties and an associated effect on the cloud albedo (Twomey effect) from MACv2-SP. Briefly, SP-05 uses the values for 2005 and SP-75 for 1975 with further details on MACv2-SP explained elsewhere (Fiedler et al., 2017; Stevens et al., 2017). The  $\tau_a$  patterns (Figures 1a and 1b) imply roughly a  $\tau_a$  reduction by a factor of 2 over the North Atlantic in SP-05 compared to SP-75.

We additionally perform two simulations for further diagnostics for the 1970s aerosol. First, this is experiment SP-75-NT, where we switch off ACI and simulate ARI only. We do so by prescribing the anthropogenic aerosol optical properties of 1975, but do not perturb the cloud droplet number concentrations. By comparison to SP-75, we separate the contributions from ACI (SP-75 minus SP-75-NT) and ARI (SP-75-NT) to the climate response. Second, we perform simulation SP-75-ATF, where we roughly quadrupled  $\tau_a$  and the associated Twomey effect. Technically, we quadruple  $\tau_a$  in the plume centers of the 1970s pattern that scales the global distribution of  $\tau_a$  and the associated Twomey effect. In essence, we obtain a stronger radiative forcing without changing the spatial pattern to gain additional confidence in our results for the contributing mechanisms, since the response in SP-75 and SP-75-ATF is qualitatively similar (not shown).

Our experiment strategy gives robust estimates of the aerosol pattern effects on climate in a contemporary atmosphere-ocean model of CMIP6. The response to anthropogenic aerosol changes are determined by calculating the difference in the mean state of new long simulations. The first 50 (100) years are removed as spin-up period before analyzing the climate (AMOC) response. The long climate estimates for every aerosol pattern make our experiment strategy comparable to performing an ensemble of 200 simulations for each aerosol pattern. This is much longer than experiments in most, if not all, previous studies on this topic and gives statistical significant results for the atmosphere and ocean response (e.g., Figures 1c-1f).

### 3. Results

#### 3.1. Global Mean SST

While there are substantial differences in the global distribution of anthropogenic aerosols in the 1970s and 2000s, the global mean SST response in the periods is similar, with a cooling by  $-0.18^{\circ}\text{C}$  relative to PI. We estimate that ACI explains more than two third of the global mean SST response to anthropogenic aerosols in our model (Table 1; SP-75 vs. SP-75-NT), despite our radiative forcing of anthropogenic aerosols associated with ACI (Fiedler et al., 2017) being relatively smaller compared to other contemporary estimates (Bellouin et al., 2020; Gryspeerdt et al., 2020). Inducing stronger aerosol effects on clouds would therefore efficiently reduce the global mean SST, all else held constant. A stronger cooling associated with stronger ACI is not implausible in light of the uncertainty (Bellouin et al., 2020) and could for instance be expected in EC-Earth, which has a more negative aerosol forcing due to the stronger ACI with MACv2-SP (Fiedler et al., 2019b). The magnitude of ACI is therefore crucial to constrain the global mean SST response, consistent with Menary et al. (2020).

#### 3.2. SST Pattern

The negative anthropogenic aerosol radiative effects (Figure S2) causes the expected northern hemisphere SST reduction in SP-75 compared to PI, but the eastern part of the sub-polar gyre in the North Atlantic responds with a SST increase (Figure 1c), consistent with other data (Dagan et al., 2020). Regional SST reductions associated with anthropogenic aerosols are at the order of  $-0.5^{\circ}\text{C}$ . In the sub-polar gyre, the SST is higher in SP-75 compared to PI by about the same magnitude, despite the negative radiative forcing of the prescribed anthropogenic aerosols (Fiedler et al., 2019b). This result is counter-intuitive since adding aerosols is expected to scatter more incoming shortwave radiation and hence to cool the surface. This is clearly not the case over the sub-polar gyre.

The mean NASST responses for the 2000s aerosol pattern is similar, with a spatially averaged NASST response of  $-0.28^{\circ}\text{C}$  in SP-75 and  $-0.27^{\circ}\text{C}$  in SP-05 relative to PI (Table 1). However, the spatial patterns of the NASST response differ between SP-75 and SP-05 (Figure 1d) for reasons discussed in the following sections. The NASST in polar regions is higher in SP-05 than in SP-75, suggesting that the 1970s–2000s reduction in  $\tau_a$  over the Atlantic has contributed to Arctic amplification. The smaller  $\tau_a$  over the North Atlantic in SP-05 is associated with weaker outgoing shortwave radiation favoring a relative warming compared to SP-75, which if it is in a classical historical simulation would act in synergy with the effect of increasing greenhouse gas emissions. Again, the SST in the eastern sub-polar gyre behaves opposite to what would be expected from the regionally reduced  $\tau_a$ . This is a clear NAWH in the eastern sub-polar gyre in SP-05 relative to SP-75.

The presence of a NAWH is qualitatively consistent with observations across different periods (e.g., Drijfhout et al., 2012; Gervais et al., 2018; Rahmstorf et al., 2015). Our experiments indicate that the regional reduction in anthropogenic aerosol burden since the 1970s to 2000s contributed to the strengthening of the NAWH, namely with a regional cooling by  $-0.5^{\circ}\text{C}$ . A role of anthropogenic aerosol for the NAWH might seem counter-intuitive, since the regional pollution reduced and therefore suggests a warming. Indeed, the radiative forcing over the North Atlantic in SP-05 is less negative than in SP-75 (Fiedler et al., 2017) and cannot directly drive the NAWH. The regional reduction in anthropogenic aerosols rather induces responses of the atmosphere and ocean that explain the behavior.

#### 3.3. Atmospheric Dynamics

We identify responses of the atmospheric conditions near the surface. Here, we use SP-75-ATF that has the same aerosol pattern and qualitatively the same responses as SP-75 (not shown), but produces stronger signals for an easier identification. Note that the aerosol effects could be larger than prescribed in SP-75 because of the uncertainty in ACI, discussed in Section 4.

Our analysis points to an increase in the zonal wind speed at 10 m across parts of the North Atlantic for SP-75-ATF relative to PI (Figure 1e). This behavior is particularly pronounced in northern hemisphere winter and consistent with the equatorward shift of the jet with larger  $\tau_a$  over the North Atlantic (Figures S3 and S4). The 10 m-wind response is consistent with the increased horizontal pressure gradient between the

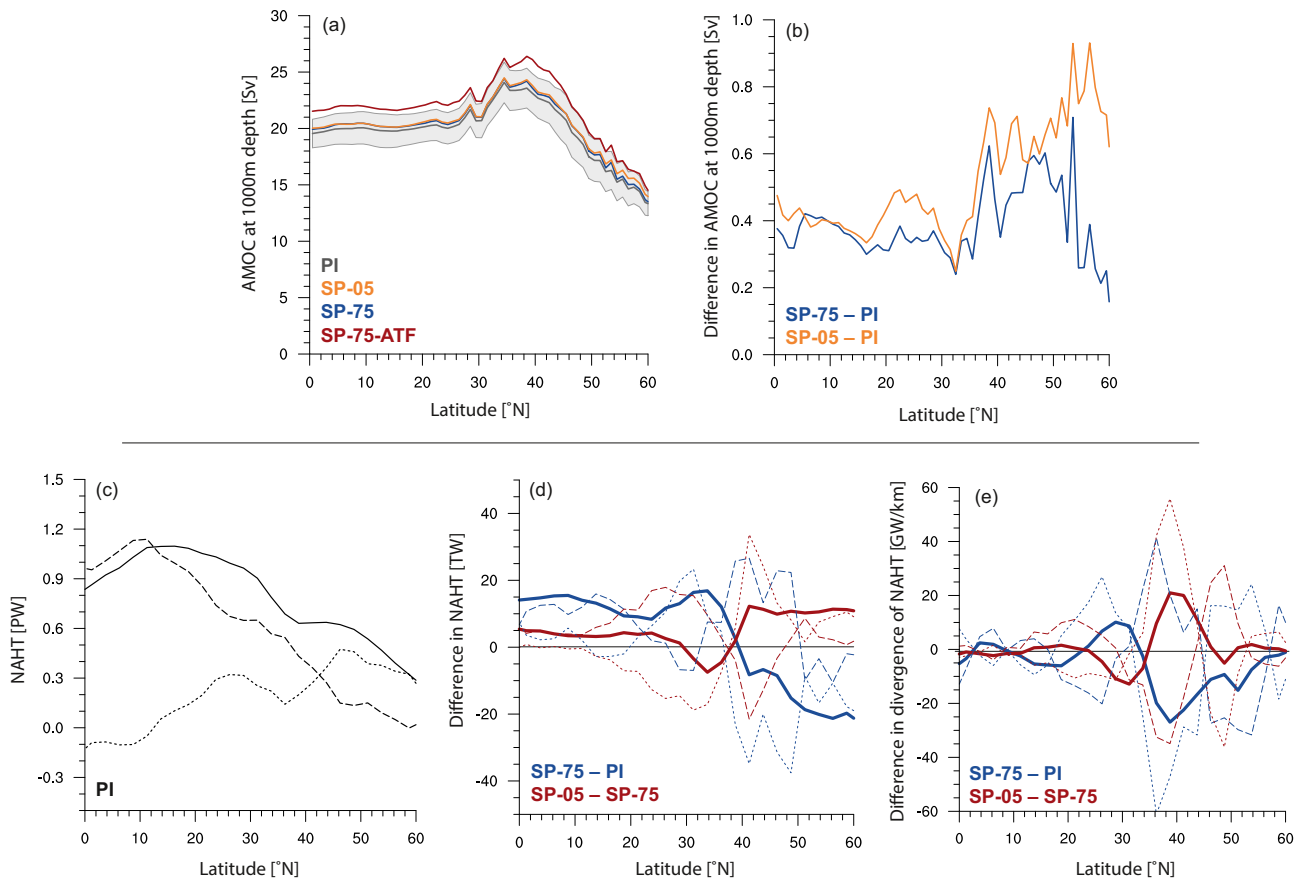


**Figure 2.** Response of the North Atlantic Ocean dynamics to anthropogenic aerosol. Shown is the response of (a–b) the Atlantic meridional overturning circulation (AMOC) at 1,000 m below the sea surface, and (c–e) the northward Atlantic heat transport (NAHT) separated into gyre (dotted) and overturning (dashed) components as (c) absolute values for PI, (d) absolute differences, and (e) differences in the divergence. The calculation of the divergence is based on NAHT data regressed onto third order polynomials to smooth variations over length scales shorter than 800 km using a filter (Savitzky & Golay, 1964).

stronger Azores High and Icelandic Low (Figure 1f). A wind and sea-level pressure response has also been diagnosed in other data (Hassan et al., 2020). The response in the mean sea-level pressure can be linked with the response of the vertical temperature profiles (Figure S5). For instance, the air cooling between the equator and 30°N acts to increase the air mass in the column leading to a pressure increase near the surface. Similarly, the NAWH over the eastern subpolar gyre induces anomalously low pressure. As a result, the horizontal pressure gradient between the Azores and higher latitudes increases, thus inducing anomalously larger mean zonal winds across the central North Atlantic. This implies more eastward stress at the ocean surface coincident with the southern branch of the sub-polar gyre. The stress induces here a strengthening of the cyclonic circulation of the gyre, thereby enhancing the northward Atlantic heat transport on the southern side of the gyre.

### 3.4. Ocean Dynamics

The SST response indicates a change in ocean dynamics. We assess the role of the subpolar gyre and the meridional overturning circulation (MOC). Both  $\tau_a$  distributions from the 1970s and 2000s are associated with a stronger Atlantic MOC (AMOC), shown in Figures 2a and 2b. The change in the magnitude of the AMOC is up to 0.4 Sv and falls within the internal variability (Figure 2a), but this does not necessarily imply that the effect of anthropogenic aerosols is negligible. Aerosol radiative effects, particularly ACI, could be stronger than in MPI-ESM1.2 (Bellouin et al., 2020; Fiedler et al., 2019b; Gryspeerdt et al., 2020; Menary et al., 2020). More negative aerosol radiative effects are expected to induce a stronger AMOC response. Take for instance the case of quadrupling aerosol radiative forcing (SP-75-ATF), where the AMOC in MPI-ESM1.2

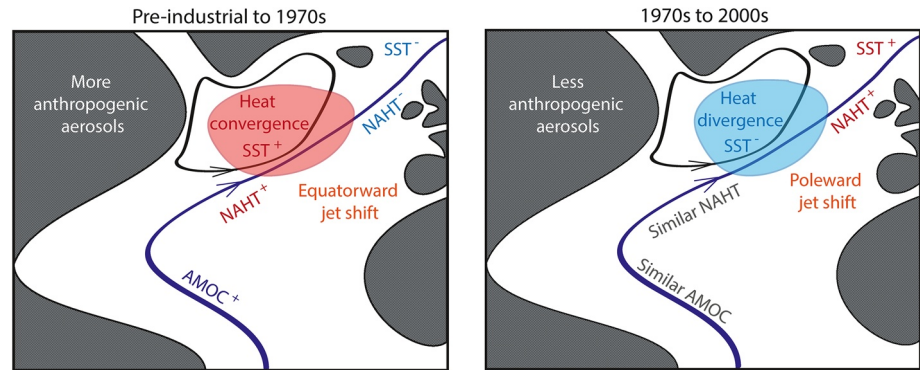


**Figure 3.** Sketch of the sea-surface temperature (SST) response to the different patterns of anthropogenic aerosols. The left (right) depicts the decrease (increase) in NASST for the 1970s (2000s) opposite to the weakening (strengthening) of the warming hole. The differences in the Atlantic Meridional Overturning Circulation (AMOC), and the Northward Atlantic Heat Transport (NAHT) are indicated. Blue line indicates the AMOC, black circular line the sub-polar gyre circulation, and dark shading land.

strengthens beyond the model-internal variability (Figure 2a). This suggests that the AMOC can respond to aerosol forcing, consistent with other data (Booth et al., 2012; Hassan et al., 2020; Menary et al., 2020).

The change in the Northward Atlantic heat transport (NAHT) explains the regionally different response of the NASST to the aerosol patterns, particularly the counter-intuitive behavior of the NAWH. For a detailed analysis, we decompose the total NAHT into the overturning and gyre components using an established method (e.g., Jungclaus et al., 2014). At lower latitudes up to roughly 40°N, the overturning component dominates the NAHT (Figure 2c). At higher latitudes, the gyre component plays a larger role in the NAHT. Similar to the AMOC, NAHT is generally stronger in both SP-75 and SP-05 compared to PI (Figure 2d) at lower latitudes where the overturning component of the NAHT dominates. Around 37°N, SP-75 has a marked maximum difference in NAHT of 20 TW compared to PI (blue solid, Figure 2d). It occurs right around where the difference in the gyre component (blue dotted) and difference in the overturning component (blue dashed) intersect and namely follows the shape of the gyre component. This behavior points to a relative convergence in NAHT that peaks around 40°N and extends to almost 60°N (blue solid, Figure 2e), and similarly is dominated by the gyre component. This regional convergence of heat is consistent with the warming in the eastern sub-polar gyre for SP-75 relative to PI.

The largest difference in the NAHT between SP-05 and SP-75 is again primarily explained by the gyre heat transport (red lines, Figure 2d). Convergence in NAHT is much weaker in SP-05 compared to SP-75, leading to a relative divergence in NAHT around 40°N (solid red, Figure 2e) dominated by the gyre component (dotted red), and therefore explains the cool anomaly in the eastern sub-polar gyre (Figure 1d). Essentially, the net heat convergence (divergence) explains the positive (negative) NASST anomaly in the eastern sub-polar gyre, in contrast to the surface cooling (warming) elsewhere in the northern hemisphere associated with pattern changes of the anthropogenic aerosols (Figures 1c and 1d). Taken together, the sub-polar gyre strongly contributes to the regionally different NASST response to the anthropogenic aerosols, in addition to the MOC that is a more important contributor than the gyre for the northward heat transport only at low latitudes.

## 4. Discussion

### 4.1. Synthesis of Dynamical Processes

Our results indicate that anthropogenic aerosols of the 1970s and its evolution through to the 2000s influence the NASST patterns. The radiative effects of anthropogenic aerosols do so by inducing changes in the fully coupled atmosphere-ocean dynamics. Figure 3 provides a conceptual view of the physical mechanisms governing the response of the NASST pattern to the aerosols of the 1970s and 2000s. The increase in anthropogenic aerosols of the 1970s relative to PI induced lower NASST by both ARI and ACI, with ACI accounting here for more than two-thirds of the reduction in NASST. Relatively lower NASST particularly over high

latitudes like the Labrador Sea and the Greenland, Iceland, and Norwegian (GIN) seas can induce more convection and thus increase the AMOC like diagnosed from our experiments and consistent with other studies (e.g., Menary et al., 2020). Our diagnostics show that the AMOC increase aligns with the increased NAHT at lower latitudes, that is, the subtropical North Atlantic.

We give evidence to reconcile the counter-intuitive response of the NAWH to aerosol patterns by analyzing the NASST response in conjunction with the dynamics of the fully coupled atmosphere-ocean system. The atmospheric temperature profile response to aerosol burden in the 1970s allows for a sea-level pressure response that enhances eastward wind stress on the southern side of the subpolar gyre. This induces increased (decreased) northward ocean heat transport to the southern (northern) side of the subpolar gyre, and thus an anomalous convergence of NAHT at the subpolar latitudes that is attributed to the gyre component of NAHT. This result points to a multi-decadal muting of the North Atlantic temperature response during high aerosol burden over the North Atlantic. The associated NAHT convergence in the sub-polar gyre counteracted the emergence of the NAWH, which one would expect from increasing greenhouse gas concentrations (Keil et al., 2020).

When anthropogenic aerosol subsequently reduced from the 1970s to the 2000s, NASST relatively increased, again with the exception of the NAWH region. Our results indicate that the NAHT over this region was anomalously divergent and thus strengthened the NAWH through anomalously lower SSTs for the 2000s relative to the 1970s. The response of the NAWH to aerosol patterns in our coupled experiments is consistent with findings based on other data (Dagan et al., 2020; Gervais et al., 2019).

#### **4.2. Role of Uncertainty in Aerosol Forcing**

All our experiments show variability in NASSTs independent of the presence of anthropogenic aerosols, but the mean climate response to the aerosol radiative effects indicates a contribution of the anthropogenic aerosol changes to the NASST patterns. The question arises how strong this contribution is. For instance, Booth et al. (2012) showed a stronger NASST response to anthropogenic aerosol changes than our model simulations. We find an AMOC increase scaling with the magnitude of the anthropogenic aerosol forcing, also suggested by others (Hassan et al., 2020; Menary et al., 2020). The AMOC increase with more aerosols is in line with the idea that the general circulation acts to weaken the larger latitudinal temperature differences, here induced by ARI and ACI. Our AMOC response falls within (outside) the typical model-internal variability of the AMOC, when the radiative effects of anthropogenic aerosols are closer to the upper (lower) bound of the spread in aerosol radiative forcing.

The uncertainty in the radiative forcing of anthropogenic aerosols translates to an uncertainty in the SST response. The CMIP5 model used by Booth et al. (2012) has a stronger anthropogenic aerosol forcing (Bellouin et al., 2011) than our CMIP6 model (Fiedler et al., 2017). Both model estimates fall within the current uncertainty for the aerosol radiative forcing (Bellouin et al., 2020). We perceive the results by Booth et al. (2012) as an estimate at the upper end of the range of responses to plausible aerosol forcing magnitudes, whereas our results should be interpreted as an estimate toward the lower bound of plausible responses to anthropogenic aerosols. We identify in our simulations a dominant contribution of the aerosol effects on clouds (ACI) to the NASST response. Namely about two thirds of our NASST response is associated with ACI (Table 1), the magnitude of which is still uncertain (Bellouin et al., 2020).

### **5. Conclusions**

We conducted 250-years long experiments with the coupled atmosphere-ocean model MPI-ESM1.2 with annually repeating aerosol properties of the 1970s and 2000s. Our results do not allow to reject the hypotheses outlined in the introduction and lead to the following conclusions:

- At least two-thirds of the global mean SST response to anthropogenic aerosols in the 1970s is associated with the magnitude of aerosol-cloud interactions, all else being equal. The degree to which aerosols and clouds interact therefore significantly contributes to the NASST response.

- For most of the North Atlantic, the response to the increased anthropogenic aerosols in the 1970s is a decrease of the NASST and a relative NASST increase from the 1970s to 2000s when the aerosol burden was reduced. These findings are qualitatively consistent with earlier studies (Booth et al., 2012; Wild, 2009).
- In the eastern subpolar gyre, the behavior is opposite to the rest of the North Atlantic. This is a warm anomaly for the 1970s aerosol pattern compared to the pre-industrial, indicating a muting of the North Atlantic warming hole, when taken together with the response to greenhouse gas concentrations (Keil et al., 2020). The anthropogenic aerosol reduction from the 1970s to 2000s is associated with a cool anomaly, thus favors a strengthening of the warming hole. These findings are consistent with other approaches (Dagan et al., 2020). For the first time, our process diagnostics quantify the anomalous NAHT convergence (divergence) arising from the gyre transport causing the response to the 1970s (2000s) aerosol pattern.
- We identify a dynamical response of the fully coupled atmosphere-ocean system to changes in the aerosol pattern. In conjunction with the response of NASSTs to increased aerosol loading, we diagnosed a consistent response of the atmospheric circulation. That is an increase in the horizontal gradient in the mean sea-level pressure, stronger near-surface zonal winds, and a latitudinal shift in the upper-tropospheric jetstream over the North Atlantic, consistent with other works (e.g., Hu & Fu, 2007; Bender et al., 2012; Allen & Ajoku, 2016; Hassan et al., 2020, see supporting information). The increase in surface eastward wind stress is coincident with the southern side of the subpolar gyre, thereby enhancing (reducing) northward ocean heat transport on the southern (northern) flank of the gyre, resulting in NAHT convergence and anomalously warm SST in the warming hole during higher aerosol burden.
- More negative aerosol radiative effects are associated with a stronger AMOC, in agreement with other studies (Hassan et al., 2020; Menary et al., 2020). Qualitatively, our findings suggest that a continued global reduction of anthropogenic aerosols, for example, as future emission of CMIP6 suggest (Fiedler et al., 2019a), would favor a decrease of the AMOC and a stronger warming hole signal, all else being equal.

We argued that the magnitude of the NASST pattern response to aerosol changes largely depends on the still poorly constrained aerosol effects on clouds. This implies that uncertainty in the radiative effects of aerosols translates to a loosely constrained response of NASSTs, as well as the response of the ocean and atmosphere circulation. This includes for instance the mean position of the jetstream over the North Atlantic, which is still biased in CMIP6 models (e.g., Priestley et al., 2020). Contrasting the warming hole of the 1970s and 2000s in these models and observations has the potential to test the plausibility of the simulated aerosol effects and to contribute to improving the model representation of circulation.

### Data Availability Statement

Data of this study are available on Zenodo (Fiedler & Putrasahan, 2021).

### Acknowledgments

The authors are grateful for the liberty to independently collaborate on this study at MPI-M and acknowledge the usage of DKRZ resources for performing the simulations. The authors thank Samira Terzenbach, Karl-Hermann Wieners, and Helmuth Haak for technical support. This work was largely funded by the Max Planck Society. S. Fiedler also acknowledges funding from the German Science Foundation (Collaborative Research Center 1211, ID: 268236062) and the German Federal Ministry for Transportation and Digital Infrastructure (Hans-Ertel-Center for Weather Research, ID: 4818DWDP5A).

### References

- Allen, R. J., & Ajoku, O. (2016). Future aerosol reductions and widening of the northern tropical belt. *Journal of Geophysical Research: Atmospheres*, 121(12), 6765–6786. <https://doi.org/10.1002/2016JD024803>
- Bellouin, N., Quaas, J., Gryspeerdt, E., Kinne, S., Stier, P., Watson-Parris, D., et al. (2020). Bounding global aerosol radiative forcing of climate change. *Reviews of Geophysics*, 58(1), e2019RG000660. <https://doi.org/10.1029/2019rg000660>
- Bellouin, N., Rae, J., Jones, A., Johnson, C., Haywood, J., & Boucher, O. (2011). Aerosol forcing in the climate model intercomparison project (CMIP5) simulations by HadGEM2-ES and the role of ammonium nitrate. *Journal of Geophysical Research*, 116, D20206. <https://doi.org/10.1029/2011JD016074>
- Bellucci, A., Mariotti, A., & Gualdi, S. (2017). The role of forcings in the twentieth-century north atlantic multidecadal variability: The 1940-75 North Atlantic cooling case study. *Journal of Climate*, 30(18), 7317–7337. <https://doi.org/10.1175/JCLI-D-16-0301.1>
- Bender, F. A.-M., Ramanathan, V., & Tselioudis, G. (2012). Changes in extratropical storm track cloudiness 1983-2008: Observational support for a poleward shift. *Climate Dynamics*, 38(9), 2037–2053. <https://doi.org/10.1007/s00382-011-1065-6>
- Booth, B. B. B., Dunstone, N. J., Halloran, P. R., Andrews, T., & Bellouin, N. (2012). Aerosols implicated as a prime driver of twentieth-century North Atlantic climate variability. *Nature*, 484. <https://doi.org/10.1038/nature10946>
- Cai, W., Bi, D., Church, J., Cowan, T., Dix, M., & Rotstayn, L. (2006). Pan-oceanic response to increasing anthropogenic aerosols: Impacts on the Southern Hemisphere oceanic circulation. *Geophysical Research Letters*, 33(21). <https://doi.org/10.1029/2006gl027513>
- Clement, A., Bellomo, K., Murphy, L. N., Cane, M. A., Mauritsen, T., Rädel, G., & Stevens, B. (2015). The Atlantic multidecadal oscillation without a role for ocean circulation. *Science*, 350(6258), 320–324. <https://doi.org/10.1126/science.aab3980>
- Cowan, T., & Cai, W. (2013). The response of the large-scale ocean circulation to 20th century Asian and non-Asian aerosols. *Geophysical Research Letters*, 40(11), 2761–2767. <https://doi.org/10.1002/grl.50587>

- Dagan, G., Stier, P., & Watson-Parris, D. (2020). Aerosol forcing masks and delays the formation of the North Atlantic warming hole by three decades. *Geophysical Research Letters*, *47*(22), e2020GL090778. <https://doi.org/10.1029/2020gl090778>
- Delworth, T. L., & Dixon, K. W. (2006). Have anthropogenic aerosols delayed a greenhouse gas-induced weakening of the North Atlantic thermohaline circulation? *Geophysical Research Letters*, *33*(2). <https://doi.org/10.1029/2005gl024980>
- Delworth, T. L., & Mann, M. E. (2000). Observed and simulated multidecadal variability in the Northern Hemisphere. *Climate Dynamics*, *16*(9), 661–676. <https://doi.org/10.1007/s003820000075>
- Drijfhout, S., van Oldenborgh, G. J., & Cimadoribus, A. (2012). Is a decline of AMOC causing the warming hole above the North Atlantic in observed and modeled warming patterns? *Journal of Climate*, *25*(24), 8373–8379. <https://doi.org/10.1175/JCLI-D-12-00490.1>
- Enfield, D. B., Mestas-Núñez, A. M., & Trimble, P. J. (2001). The Atlantic Multidecadal Oscillation and its relation to rainfall and river flows in the continental U.S. *Geophysical Research Letters*, *28*(10), 2077–2080. <https://doi.org/10.1029/2000GL012745>
- Eyring, V., Bony, S., Meehl, G. A., Senior, C. A., Stevens, B., Stouffer, R. J., & Taylor, K. E. (2016). Overview of the coupled model intercomparison project phase 6 (CMIP6) experimental design and organization. *Geoscientific Model Development*, *9*(5), 1937–1958. <https://doi.org/10.5194/gmd-9-1937-2016>
- Fiedler, S., Kinne, S., Huang, W. T. K., Räisänen, P., O'Donnell, D., Bellouin, N., et al. (2019b). Anthropogenic aerosol forcing - insights from multiple estimates from aerosol-climate models with reduced complexity. *Atmospheric Chemistry and Physics*, *19*, 6821–6841. <https://doi.org/10.5194/acp-19-6821-2019>
- Fiedler, S., & Putrasahan, D. (2021). *Model simulation data for climate response to anthropogenic aerosol pattern of 1970s and 2000s*. Zenodo. <https://doi.org/10.5281/zenodo.4565589>
- Fiedler, S., Stevens, B., Gidden, M., Smith, S. J., Riahi, K., & van Vuuren, D. (2019a). First forcing estimates from the future CMIP6 scenarios of anthropogenic aerosol optical properties and an associated Twomey effect. *Geoscientific Model Development*, *12*, 989–1007. <https://doi.org/10.5194/gmd-12-989-2019>
- Fiedler, S., Stevens, B., & Mauritsen, T. (2017). On the sensitivity of anthropogenic aerosol forcing to model-internal variability and parameterizing a Twomey effect. *Journal of Advances in Modeling Earth Systems*, *9*(9), 1325. <https://doi.org/10.1002/2017MS000932>
- Gervais, M., Atallah, E., Gyakum, J. R., & Tremblay, L. B. (2016). Arctic air masses in a warming world. *Journal of Climate*, *29*(7), 2359–2373. <https://doi.org/10.1175/JCLI-D-15-0499.1>
- Gervais, M., Shaman, J., & Kushnir, Y. (2018). Mechanisms Governing the Development of the North Atlantic Warming Hole in the CESM-LE Future Climate Simulations. *Journal of Climate*, *31*(15), 5927–5946. <https://doi.org/10.1175/JCLI-D-17-0635.1>
- Gervais, M., Shaman, J., & Kushnir, Y. (2019). Impacts of the North Atlantic Warming Hole in Future Climate Projections: Mean Atmospheric Circulation and the North Atlantic Jet. *Journal of Climate*, *32*(10), 2673–2689. <https://doi.org/10.1175/JCLI-D-18-0647.1>
- Gryspeerd, E., Mülmenstädt, J., Gettelman, A., Malavelle, F. F., Morrison, H., Neubauer, D., et al. (2020). Surprising similarities in model and observational aerosol radiative forcing estimates. *Atmospheric Chemistry and Physics*, *20*(1), 613–623. <https://doi.org/10.5194/acp-20-613-2020>
- Hassan, T., Allen, R. J., Liu, W., & Randles, C. (2020). Anthropogenic aerosol forcing of the AMOC and the associated mechanisms in CMIP6 models. *Atmospheric Chemistry and Physics Discussions*, 1–28. <https://doi.org/10.5194/acp-2020-769>
- Hu, Y., & Fu, Q. (2007). Observed poleward expansion of the Hadley circulation since 1979. *Atmospheric Chemistry and Physics*, *7*(19), 5229–5236. <https://doi.org/10.5194/acp-7-5229-2007>
- IPCC. (2013). *Climate change 2013: The physical science basis. contribution of working group I to the fifth assessment report of the intergovernmental panel on climate change, 14771496*. Annex v: Contributors to the IPCC WG1 fifth assessment report [Book Section]. Cambridge UK and New York, NY, USA: Cambridge University Press. Retrieved from [www.climatechange2013.org](http://www.climatechange2013.org)
- Jungclaus, J. H., Lohmann, K., & Zanchettin, D. (2014). Enhanced 20th-century heat transfer to the Arctic simulated in the context of climate variations over the last millennium. *Climate of the Past*, *10*(6), 2201–2213. <https://doi.org/10.5194/cp-10-2201-2014>
- Keil, P., Mauritsen, T., Jungclaus, J., Hedemann, C., Olonscheck, D., & Ghosh, R. (2020). Multiple drivers of the north Atlantic warming hole. *Nature Climate Change*, *10*(7), 667–671. <https://doi.org/10.1038/s41558-020-0819-8>
- Kim, W. M., Yeager, S. G., & Danabasoglu, G. (2018). Key role of internal ocean dynamics in Atlantic multidecadal variability during the last half century. *Geophysical Research Letters*, *45*(24), 13449–13457. <https://doi.org/10.1029/2018GL080474>
- Knight, J. R., Allan, R. J., Folland, C. K., Vellinga, M., & Mann, M. E. (2005). A signature of persistent natural thermohaline circulation cycles in observed climate. *Geophysical Research Letters*, *32*(20). <https://doi.org/10.1029/2005GL024233>
- Maher, N., Milinski, S., Suarez-Gutierrez, L., Botzet, M., Dobrynin, M., Kornbluh, L., et al. (2019). The Max Planck institute grand ensemble: Enabling the exploration of climate system variability. *Journal of Advances in Modeling Earth Systems*, *11*(7), 2050–2069. <https://doi.org/10.1029/2019MS001639>
- Marshall, J., Scott, J. R., Armour, K. C., Campin, J.-M., Kelley, M., & Romanou, A. (2015). The ocean's role in the transient response of climate to abrupt greenhouse gas forcing. *Climate Dynamics*, *44*(7), 2287–2299. <https://doi.org/10.1007/s00382-014-2308-0>
- Mauritsen, T., Bader, J., Becker, T., Behrens, J., Bittner, M., Brokopf, R., et al. (2019). Developments in the MPI-M Earth System Model version 1.2 (MPI-ESM 1.2) and its response to increasing CO2. *Journal of Advances in Modeling Earth Systems*, *11*, 998–1038. <https://doi.org/10.1029/2018MS001400>
- Menary, M. B., Robson, J., Allan, R. P., Booth, B. B. B., Cassou, C., Gastineau, G., et al. (2020). Aerosol-Forced AMOC Changes in CMIP6 Historical Simulations. *Geophysical Research Letters*, *47*(14), e2020GL088166. <https://doi.org/10.1029/2020gl088166>
- Otter, O. H., Bentsen, M., Drange, H., & Suo, L. (2010). External forcing as a metronome for Atlantic multidecadal variability. *Nature Geoscience*, *3*, 688–694. <https://doi.org/10.1038/ngeo955>
- Priestley, M. D. K., Ackerley, D., Catto, J. L., Hodges, K. I., McDonald, R. E., & Lee, R. W. (2020). An overview of the extratropical storm tracks in CMIP6 historical simulations. *Journal of Climate*, *33*(15), 6315–6343. <https://doi.org/10.1175/JCLI-D-19-0928.1>
- Rahmstorf, S., Box, J. E., Feulner, G., Mann, M. E., Robinson, A., Rutherford, S., & Schaffernicht, E. J. (2015). Exceptional twentieth-century slowdown in Atlantic ocean overturning circulation. *Nature Climate Change*, *5*(5), 475–480. <https://doi.org/10.1038/nclimate2554>
- Savitzky, A., & Golay, M. J. E. (1964). Smoothing and differentiation of data by simplified least squares procedures. *Analytical Chemistry*, *36*(8), 1627–1639. <https://doi.org/10.1021/ac60214a047>
- Stevens, B., Fiedler, S., Kinne, S., Peters, K., Rast, S., Mücke, J., et al. (2017). MACv2-SP: A parameterization of anthropogenic aerosol optical properties and an associated Twomey effect for use in CMIP6. *Geoscientific Model Development*, *10*(1), 433–452. <https://doi.org/10.5194/gmd-10-433-2017>
- Trenberth, K. E., & Shea, D. J. (2006). Atlantic hurricanes and natural variability in 2005. *Geophysical Research Letters*, *33*(12). <https://doi.org/10.1029/2006GL026894>
- Wang, C., Dong, S., Evan, A. T., Foltz, G. R., & Lee, S.-K. (2012). Multidecadal covariability of North Atlantic sea surface temperature, African dust, Sahel rainfall, and Atlantic hurricanes. *Journal of Climate*, *25*(15), 5404–5415. <https://doi.org/10.1175/JCLI-D-11-00413.1>

- Wild, M. (2009). Global dimming and brightening: A review. *Journal of Geophysical Research*, 114(D10). <https://doi.org/10.1029/2008JD011470>
- Woollings, T., Gregory, J. M., Pinto, J. G., Meyers, M., & Brayshaw, D. J. (2012). Response of the North Atlantic storm track to climate change shaped by ocean-atmosphere coupling. *Nature Geoscience*, 5(5), 313–317. <https://doi.org/10.1038/ngeo1438>
- Zhang, L., & Wang, C. (2013). Multidecadal North Atlantic sea surface temperature and Atlantic meridional overturning circulation variability in CMIP5 historical simulations. *Journal of Geophysical Research*, 118(10), 5772–5791. <https://doi.org/10.1002/jgrc.20390>